

Electrochemical behaviour of Vanadium(V) on electrochemically synthesized magnetite film electrodes

*Sergio G. Dabrowski, Mabel B. Tudino and Fernando V. Molina**

Instituto de Química Física de Materiales, Ambiente y Energía (INQUIMAE), Facultad de Ciencias Exactas y Naturales, Universidad de Buenos Aires, Buenos Aires, Argentina.

CORRESPONDING AUTHOR: Fernando V. Molina. Instituto de Química Física de Materiales, Ambiente y Energía (INQUIMAE), Facultad de Ciencias Exactas y Naturales, Universidad de Buenos Aires. Ciudad Universitaria, Pabellon II, piso 1, C1428EHA Buenos Aires, Argentina.

Phone: +54-11-4576-3378/80 ext 230

FAX: +54-11-4576-3341

E-mail: fmolina@qi.fcen.uba.ar

ABSTRACT:

In this work, the electrochemical response of Vanadium(V) species on magnetite film electrodes is investigated. Magnetite is deposited electrochemically on glassy carbon electrodes, with an intermediate layer of poly(thiophene) to avoid water infiltration. These electrodes show good reproducibility and stability up to pH = 2.0. Mononuclear V(V) species show low electroactivity on this surface. Cyclic voltammetry at low V(V) concentration shows that it is electroactive only at pH < 3. i.e. as VO₂⁺. A single reduction peak is observed at ~ -0.7 V vs SCE (at 50 mV s⁻¹), and an oxidation one at ~ 0.5 V vs SCE, indicating high irreversibility of the V(V)/V(IV) couple; these peaks are found to be solution phase reactions. These features are interpreted in terms of mononuclear V species. At higher V concentrations, where polymeric V(V) species are dominant, a somewhat higher electroactivity is observed, with two reduction peaks and two/three oxidation peaks.

Keywords: conducting polymer; iron oxide; cyclic voltammetry

1. INTRODUCTION

Magnetite is unique among the iron oxides because of its conducting and magnetic properties [1]; its magnetism is the basis of a number of simple methods for removal of arsenic, a well known toxic element, from natural waters. These methods are generally based on the adsorption of As anionic species onto the oxide following extraction of the Fe_3O_4 particles via a magnetic field [2–5]. Vanadium is another element commonly found in groundwater, and is potentially harmful to humans [6]; moreover, it often correlates positively with arsenic [7]. Vanadium, usually found as anionic species, can also adsorb onto iron oxides, and V removal using a Fe oxohydroxide has been reported [8,9]; thus V, besides its own toxicity, is a potential interference in As removal using iron oxides. Consequently, the knowledge of the interaction of V species with iron oxo- or oxohydroxides, including redox behaviour, is important to understand the competence of As and V and ultimately such remediation methods.

There are very few studies of V adsorption onto iron oxides. Jin et al. [10,11] studied by density functional theory (DFT) the adsorption of V onto idealized hematite crystal faces, concluding that it forms mainly threefold bonds with O atoms. Peacock and Sherman [12] investigated experimentally and theoretically the adsorption of V(V) species onto goethite; EXAFS measurements indicated the presence of bidentate inner-sphere surface complexes, attributed to corner-sharing species through DFT ab-initio calculations. On the basis of such results a surface complexation model was proposed that predicted satisfactorily the adsorption edge experiments.

The electrochemistry of Vanadium has received more attention. This element has a complex redox-pH behaviour (Fig. 1) [13] which reflects in its electrochemical response. Israel and Meites [14] studied by polarography, amperometry and chronocoulometry the reactions between V(II), V(III), V(IV) and V(V) species, concluding that the formation of polynuclear species led to the complex behaviour observed. Goto and Ishii [15] studied the chronopotentiometry of V(V) in phosphoric acid solutions, reporting the presence of two couples, V(V)/V(IV) and V(IV)/V(III), reversible and irreversible, respectively. The

V(III)/V(II) couple was investigated by several authors [14,16,17] and generally considered reversible; the V(IV)/V(III) couple, on the other hand, was reported to be reversible on Pt but irreversible on Hg [18]. The electrochemical response of metallic V has also been studied [19,20]. There are no reports, to the best of our knowledge, on the electrochemistry of V on non-metallic surfaces.

The electrochemistry of magnetite has been studied quite extensively, mostly in connection with its role in iron passivity and corrosion; also, the oxygen evolution on Fe₃O₄ surfaces has received attention in the literature [21,22 and references therein]. Albeit most studies have been conducted in alkaline media, in acidic media it was found, at pH = 1, a relatively low polarization current between oxygen evolution at about -1.9 V and hydrogen evolution at ~ -0.6 V, both vs NHE [23].

The electric conductivity of magnetite allows its use as substrate for electrochemical measurements.

Thus, it can be expected that the interaction between Fe₃O₄ and V can be examined through electrochemical methods.

Here, a voltammetric study of V(V) electrochemical response on magnetite film electrodes (MFE) is reported, with the aim of investigate the electroactivity of magnetite towards vanadium. Fe₃O₄ films are grown electrochemically. For solid ion selective electrodes, it was reported that a layer of a hydrophobic conducting polymer improved stability by avoiding the formation of a thin water layer in the electrode/film interphase [24]. Therefore, the same approach was taken in the present work: the electrochemically formed Fe₃O₄ films are deposited on polythiophene (PT) films, in turn electrochemically grown on glassy carbon (GC) electrodes.

2. EXPERIMENTAL

2.1. Chemicals and materials

AR grade chemicals and high purity water from a Milli-Q system were employed throughout. V(V) was added in the form of ammonium metavanadate. The electrochemical experiments were conducted in a

three electrode cell, with working and auxiliary electrodes placed in the same compartment; the working electrodes were 0.3 cm diameter glassy carbon (GC) disks, polished with alumina of decreasing sizes up to 0.3 μm , cleaned in an ultrasonic bath with acetone, thoroughly rinsed with high purity water and dried in air. The reference electrode was a saturated calomel electrode (SCE); all potentials are referred to it. The counterelectrode was a Pt foil. A Teq-04 (S. Sobral, Buenos Aires, Argentina) potentiostat under computer control was employed in all the experiments.

2.2. Electropolymerization of thiophene

The PT base films were synthesized galvanostatically following Bobacka et al. [25]. The GC disks were immersed in a 0.1 M thiophene + 0.1 M LiClO_4 propylene carbonate solution. A 1.43 mA cm^{-2} current was applied for 80 s with the GC electrode acting as anode; after that the electrode was removed and rinsed thoroughly with high purity water, and allowed to dry in air.

2.3. Magnetite film formation

The Fe_3O_4 films were also obtained galvanostatically, following Abe and Tamaura [26]. The cell was initially filled with ultrapure water, degassed with 99.98 % N_2 and heated to 80 $^\circ\text{C}$ in a thermostatic bath; then, FeSO_4 , $\text{NH}_4\text{CH}_3\text{COO}$ and KOH are added so as to reach concentrations of 0.028 M, 0.026 and 0.057 M, respectively. Immediately, an anodic constant current of 0.25 mA cm^{-2} is applied for a 2 h period. Finally, the electrode is removed and carefully rinsed with water. A dark, homogeneous surface is observed. The procedure is reproducible, resulting in electrodes with good conductivity.

2.4. Film characterization

Microscopical observation was performed on MFEs grown with the procedure given above on ITO surfaces, so as to be fitted into the SEM chamber. The base surfaces, the PT films and the final magnetite films were observed by scanning electron microscopy (SEM) with a Zeiss Supra 40 Gemini microscope.

The formation of Fe₃O₄ was verified by grazing incidence X-ray diffraction (GIXRD). A Siemens D5000 diffractometer was employed, at an angle of 2°, 0,02° theta steps and 5 s per step; Cu-K α radiation was employed.

Further characterization was performed through ATR-FTIR spectra determination of the base surface, PT and magnetite films, using a Nicolet 8700 equipment fitted with a diamond crystal ATR accessory.

The acid-base behaviour of Fe₃O₄ films was characterized by titration with 0.1 M KOH solution in KNO₃ 0.01 M supporting electrolyte, after addition of HNO₃ to bring the pH to a sufficient acidic media, simultaneously recording the solution pH and the potential difference, ΔE , against a saturated calomel electrode (SCE). Numerical fitting of the results is performed with the aid of the Mathematica package (Wolfram Research Inc., www.wolfram.com).

2.5. Electrochemical experiments

The film electrodes were placed in a 0.01 M KNO₃ solution adjusted to the desired pH values by KOH or HNO₃ additions. Nitrogen gas (99.98 %) was bubbled in the solution before all measurements, and kept passing over the liquid afterward, to exclude oxygen gas. Blank voltammograms were recorded in this supporting electrolyte solution; V(V) was added in the form of NH₄VO₃. Unless otherwise noted, the sweep rate, ν , was 50 mV s⁻¹.

3. RESULTS AND DISCUSSION

3.1 Microscopical observation

Fig. 2 shows typical SEM images of the magnetite films in the preparation stages. Fig 1a shows the original ITO surface, whereas Fig. 2b shows an ITO film with the PT film on top: a darker image is observed, indicating a higher electron absorption. Fig 3c shows a magnetite film, revealing the presence

of globule-like surface structures; the bright areas at the borders are larger globular structures. It is clearly seen that the MFE structure is not influenced by the underlying surface morphology.

3.2 GIXRD results

Fig. 3 shows the grazing incidence XRD patterns found for the base ITO surface and the film formed. The magnetite main diffraction lines are identified, indicating that the film is effectively Fe₃O₄.

3.3 FTIR spectra

Fig. 4 shows the ATR-FTIR spectra of the bare ITO surface, this surface with the PT film, and of the complete MFE. In the second case, the spectrum shows little differences with the bare surface because the PT film is very thin, which is also apparent in the SEM images, Fig. 2. In the last spectrum, the magnetite main band at 537.6 cm⁻¹ is clearly observed, thus confirming the composition of this film.

3.4 Surface titration

Fig. 5 (squares) shows the results of the surface potential of the MFE measured against the SCE as a function of medium pH. A typical response of oxide surfaces is observed; the point of zero charge, pzc, is located at about pH = 8.2.

The acid-base behaviour of oxide surfaces is generally interpreted in terms of diverse surface complexation models [27,28]; here we will analyze the experimental results of Fig. 5 using the 1-pK diffuse layer model (1pK-DL) [29]. The acid-base equilibrium is assumed to be established by the single reaction:



where FeO represents a surface site. This reaction responds to the equilibrium expression

$$K_{int} e^{\frac{F\psi}{RT}} = \frac{\Gamma_{\text{FeO}^{-1/2}} \{H^+\}}{\Gamma_{\text{FeOH}^{+1/2}}} \quad (2)$$

where K_{int} is the intrinsic equilibrium constant, ψ is the surface electrical potential, Γ is surface concentration and $\{H^+\}$ is the proton activity in solution. F , R and T have their usual meaning. The surface charge is given by:

$$\sigma = \frac{F}{2} (\Gamma_{\text{FeOH}^{+1/2}} - \Gamma_{\text{FeO}^{-1/2}}) \quad (3)$$

and the surface mass balance is given by

$$\Gamma_T = \Gamma_{\text{FeOH}^{+1/2}} + \Gamma_{\text{FeO}^{-1/2}} \quad (4)$$

with Γ_T being the total concentration of surface sites. Finally, the Guy-Chapman equation is assumed to hold for the charge-potential relationship:

$$\sigma = \sqrt{8I\varepsilon_r\varepsilon_0RT} \sinh\left(\frac{F\psi}{2RT}\right) \quad (5)$$

where I is the ionic strength (molar units), ε_r is the relative water dielectric constant and ε_0 the vacuum permittivity. The measured potential difference is assumed to differ from ψ by a constant term ψ_r containing the reference electrode potential, junction potentials, etc.:

$$\Delta E = \psi - \psi_r \quad (6)$$

The model defined by eq. (1)-(6) is fitted to the experimental data taking K_{int} , Γ_T and ψ_r as parameters, resulting in the dashed curve of Fig. 5: a very good fitting is obtained. The resulting parameters are $K_{int} = 6.42 \times 10^{-9}$, $\Gamma_T = 3.89 \times 10^{-7} \text{ mol m}^{-2}$ and $\psi_r = -0.3 \text{ mV}$. In the 1pk-DL model, the intrinsic constant is directly related to the pzc, being $\text{pzc} = -\log K_{int} = 8.19$ as observed in Fig. 5. This value of pzc is within the range commonly found for iron oxides [30], albeit for magnetite lower values are usually found. The

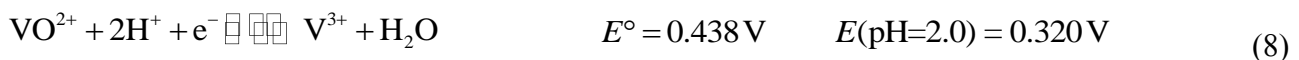
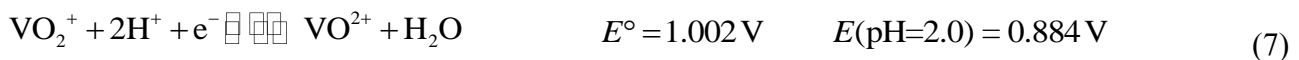
surface site concentration, as detected in the acid-base titration is noticeably lower than solid oxide electrodes, resulting of about 0.25 nm^{-2} . This indicates that this surface has a low concentration of OH active sites.

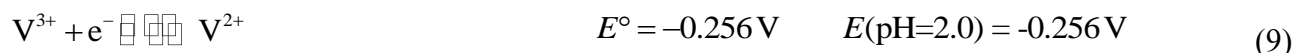
3.5 Voltammetric response

MFEs grown with a PT intermediate layer shown good, stable electrochemical response; in the absence of such layer, an erratic response was often observed. When a MFE is cycled in support electrolyte, a rather featureless voltammogram is observed between -0.85 and 1.45 V (Fig. 6, dotted line). A stable, essentially capacitive response is achieved after few cycles, typically 5-10; this response is almost independent of pH, being stable up to pH = 2.0. This is in qualitative agreement with the results of Allen et al. [23]. In the presence of V(V), no response is observed between pH = 9.0 and 4.0. At pH ~ 3 some peaks are distinguished over the base curve, and finally at pH = 2.0 clear peaks, one cathodic at $E \approx -0.7$ V and one anodic, at $E \approx 0.5$ V are found; these peaks grow consistently as the V(V) concentration is increased (Fig. 6, solid line). When mechanical stirring is applied (Fig. 6, dashed line), the cathodic current peak increases, whereas the anodic one decreases, indicating solution phase electrode reactions: for reduction, stirring increases the transport of V(V) to the surface, whereas in the opposite reaction the effect is to remove the reduced products. It was also verified that the cathodic peak currents have a linear dependence with the square root of ν .

At V(V) concentrations below 1 mM, precipitated and polynuclear V_n (with $n > 2$) species are absent (Fig. 1) and at pH = 2 and above, the dominant species, thus the electroactive one in this case, is VO_2^+ .

The relevant reactions at pH = 2, according to Post and Robins [13] in these conditions are:



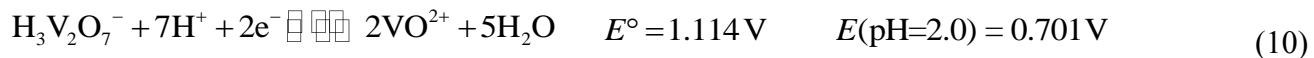


where the potentials at the right are estimated at pH = 2 and equal concentrations of the oxidized and reduced species; clearly at the potential of the cathodic peak all these values are largely exceeded, thus it can be concluded that V(V) has a highly irreversible (high overpotential) behaviour on magnetite surfaces. According to the literature, the couple V(V)/V(IV) is generally irreversible, the V(IV)/V(III) one is reversible on some surfaces (such as Pt) and irreversible on others (as Hg); finally, the V(III)/V(II) couple is often found to be reversible [14–18,31].

To gain insight in the voltammetric response, experiments changing the anodic limit in a quiescent solution were performed (Fig. 7). It is observed that the reduction current at the cathodic end of the scan decreases as the anodic potential limit decreases. In the absence of stirring, the replenishing of the V(V) species is slow; if the scan is reversed before reaching the oxidation potential range, less reactant is found and so the reduction current is lower than in the full scan. When the scan reaches the anodic peak potential, the reduction current increases noticeably. However, there is still some more increase of the cathodic peak current upon reaching the anodic limit of 1.45 V vs SCE; further increase of this limit produces essentially the same results. Based on these observations, and the Nernst potentials of reactions (7)-(9), we propose that in the cathodic peak V(V) is reduced to V(IV) and simultaneously further reduced to a lower oxidation state, either V(III) or (II). In the anodic scan, this last species is reoxidized to V(IV) (because the anodic peak potential is lower than the thermodynamic V(V)/V(IV) one), and further oxidized near to the anodic limit, where the current for this process presumably is superimposed to other reactions taking place at this high potential value, such as substrate oxidation and/or oxygen evolution.

The fact that at pH > 2 no reaction is observed in the conditions of this study indicates that other V(V) species have very high reduction overpotentials. For instance, the main species in the pH range of 3-6 is

$\text{H}_3\text{V}_2\text{O}_7^-$, which is reduced as



thus it would be expected to be reduced in the potential range studied. It can be concluded that V(V) species at low concentrations (< 1 mM) have low, if any, reactivity on Fe_3O_4 surfaces.

Fig 8 shows the response observed at higher V(V) concentrations. Here, there is more electrochemical activity than at low concentrations. At $v \leq 100 \text{ mV s}^{-1}$ two cathodic and three anodic peaks are observed; at higher sweep rates, the first two anodic peaks merge into a single one. The current of the other peaks show a linear dependence with $v^{1/2}$, indicating also solution phase reactions. The thermodynamically stable species in these conditions is $\text{H}_2\text{V}_{10}\text{O}_{28}^{4-}$ (Fig. 1). Unfortunately, there is a lack of information about the redox behaviour of polymeric V species. The thermodynamic data of Post and Robins [13] only include the reduction of such species to $\text{V}_2\text{O}_4(\text{s})$, and of this one to $\text{V}_2\text{O}_3(\text{s})$:



Reactions (11) and (12) could in principle be consistent with the two cathodic peaks observed; however, in the absence of knowledge on the electrochemistry of polyvanadates, this point cannot be discussed further.

Concluding, at V concentrations below 1 mM (which is the range relevant from an environmental point of view) there is little V(V) electrochemical activity, showing response only at far cathodic potentials. This behaviour is interpreted in terms of the mononuclear V redox couples. At higher concentrations, polynuclear V(V) species show more reactivity.

ACKNOWLEDGMENTS: The authors acknowledge financial support from de Universidad de Buenos Aires (grant 20020130100035BA), the Consejo Nacional de Investigaciones Científicas y Técnicas (CONICET), Argentina (grant PIP F57269), and the Agencia Nacional de Promoción Científica y Tecnológica, Argentina (grant PICT 2014-2289). M.B.T. and F.V.M are members of the Carrera del Investigador Científico of CONICET. F. V. M. remembers warmly the unforgettable experience of being working under Roger Parsons as a postdoc fellow in 1988-1989. We all will miss him greatly.

FIGURE CAPTIONS

Fig. 1 (a) The potential/pH diagram for the vanadium-water system at 298.15 K and total V concentration of 0.01 m; (b) Log(total concentration) vs pH diagram for the V(V) system at 298.15 K. Reprinted from Ref [13], with permission from Elsevier. Copyright Elsevier 1976.

Fig. 2. SEM images of a magnetite film electrode preparation stages: (a) underlying ITO surface, (b) the ITO with PT film, and (c) the Fe₃O₄ film surface.

Fig. 3. Grazing incidence XRD patterns of the magnetite and of the underlying ITO surface. The main Fe₃O₄ diffraction lines are indicated.

Fig. 4. ATR-FTIR spectra of the bare ITO surface, the surface with the PT film, and surface with PT and Fe₃O₄ films.

Fig. 5. Surface potential as a function of solution pH for magnetite film electrodes in 0.01 M KNO₃.

Fig. 6. Voltammograms of the MFE in 0.1 M KNO₃ at pH = 2.0, in the absence (.....) and presence of V(V), in a static solution (___) and with magnetic stirring applied (- - -). $\nu = 50 \text{ mV s}^{-1}$.

Fig. 7. The voltammetric response of a 0.31 mM V(V) solution in 0.1 M KNO₃ at pH = 2.0, at different

anodic scan limits. $\nu = 50 \text{ mV s}^{-1}$.

Fig. 8. Voltammetric response of a MFE in a 0.1 M V(V) + 0.1 M KNO₃ solution at pH = 2.0 and different sweep rates.

REFERENCES

- [1] E. Wilson, E.F. Herroun, Proc. R. Soc. Lond. A 105 (1924) 334–345.
- [2] H.J. Shipley, S. Yean, A.T. Kan, M.B. Tomson, Environmental Toxicology and Chemistry 28 (2009) 509–515.
- [3] S.R. Chowdhury, E.K. Yanful, Journal of Environmental Management 91 (2010) 2238–2247.
- [4] S.-C. Chang, Y.-H. Yu, C.-H. Li, C.-C. Wu, H.-Y. Lei, International Journal of Environmental Research and Public Health 9 (2012) 3711–3723.
- [5] S. Kango, R. Kumar, Environ Monit Assess 188 (2016) 60.
- [6] J. Taylor, S. Keith, L. Cseh, L. Ingerman, L. Chappell, J. Rhoades, A. Hueber, Toxicological Profile for Vanadium, Public Health Service Agency for Toxic Substances and Disease Registry, USA, Atlanta, Georgia, 2012.
- [7] P.L. Smedley, H.B. Nicolli, D.M.J. Macdonald, A.J. Barros, J.O. Tullio, Applied Geochemistry 17 (2002) 259–284.
- [8] H. Sharififard, M. Soleimani, RSC Adv. 5 (2015) 80650–80660.
- [9] H. Sharififard, M. Soleimani, F.Z. Ashtiani, Desalination and Water Treatment 57 (2016) 15714–15723.
- [10] J. Jin, X. Ma, C.-Y. Kim, D.E. Ellis, M.J. Bedzyk, Surface Science 601 (2007) 3082–3098.
- [11] J. Jin, X. Ma, C.-Y. Kim, D.E. Ellis, M.J. Bedzyk, Surface Science 601 (2007) 4571–4581.
- [12] C.L. Peacock, D.M. Sherman, Geochimica et Cosmochimica Acta 68 (2004) 1723–1733.
- [13] K. Post, R.G. Robins, Electrochimica Acta 21 (1976) 401–405.
- [14] Y. Israel, L. Meites, Journal of Electroanalytical Chemistry (1959) 8 (1964) 99–119.
- [15] M. Goto, D. Ishii, Journal of Electroanalytical Chemistry and Interfacial Electrochemistry 36 (1972) 1–10.
- [16] Z. El Abbassi, S. Belcadi, J.J. Rameau, Electrochimica Acta 31 (1986) 1467–1472.
- [17] W. Gorski, Z. Galus, Electrochimica Acta 34 (1989) 543–549.

- [18] L. Nucci, G. Raspi, *Journal of Electroanalytical Chemistry and Interfacial Electrochemistry* 36 (1972) 499–502.
- [19] R.D. Armstrong, M. Henderson, *Journal of Electroanalytical Chemistry and Interfacial Electrochemistry* 26 (1970) 381–386.
- [20] S. Hornkjøl, I.M. Hornkjøl, *Electrochimica Acta* 36 (1991) 577–580.
- [21] E.R. Vago, E.J. Calvo, *Journal of Electroanalytical Chemistry* 339 (1992) 41–67.
- [22] P.A. Castro, E.R. Vago, E.J. Calvo, *J. Chem. Soc., Faraday Trans. 92* (1996) 3371–3379.
- [23] P.D. Allen, N.A. Hampson, G.J. Bignold, *Journal of Electroanalytical Chemistry and Interfacial Electrochemistry* 111 (1980) 223–233.
- [24] J. Sutter, A. Radu, S. Peper, E. Bakker, E. Pretsch, *Analytica Chimica Acta* 523 (2004) 53–59.
- [25] J. Bobacka, M. McCarrick, A. Lewenstam, A. Ivaska, *Analyst* 119 (1994) 1985–1991.
- [26] M. Abe, Y. Tamaura, *Journal of Applied Physics* 55 (1984) 2614–2616.
- [27] J. Westall, H. Hohl, *Advances in Colloid and Interface Science* 12 (1980) 265–294.
- [28] K.F. Hayes, G. Redden, W. Ela, J.O. Leckie, *J. Colloid Interf. Sci.* 142 (1991) 448–469.
- [29] J. Lützenkirchen, *Environ. Sci. Technol.* 32 (1998) 3149–3154.
- [30] M. Kosmulski, *Surface Charging and Points of Zero Charge*, 1st ed., CRC Press, Boca Raton, FL, 2009.
- [31] S.M. Taylor, A. Pătru, D. Streich, M. El Kazzi, E. Fabbri, T.J. Schmidt, *Carbon* 109 (2016) 472–478.